A Comparison of an Interior Permanent Magnet and Copper Rotor Induction Motor in a Hybrid Electric Vehicle Application

James Goss, Mircea Popescu, Dave Staton

***Abstract*— this paper compares a permanent magnet motor to an induction motor in a hybrid electric vehicle application. The comparison considers replacing an existing 50kW Interior Permanent Magnet (IPM) motor with a copper-rotor induction motor (CR-IM). The 2004 Toyota Prius Hybrid system is used as the baseline for the analysis. The size, weight and cost of the two topologies are compared and the difference in lifetime energy use over various drive cycles is analysed. Additional considerations including the impact on battery sizing and the inverter VA rating are also considered and discussed.**

***Index Terms*— Hybrid Vehicle, Copper Rotor, Lifetime Energy**

I. INTRODUCTION

Permanent magnet electrical machines are typically the preferred choice in automotive traction applications due to their good torque density and high efficiency. However the price of these motors is often unacceptable for the automotive market and the fluctuation in the price of rare earth permanent magnets generates uncertainty and prohibits long term design planning. An induction motor topology offers a lower cost solution however their comparative lower efficiency, power density and power factor is less desirable. This paper attempts to quantify these aspects and assess any trade-offs by comparing a copper rotor induction motor and an interior permanent magnet motor in a hybrid electric vehicle application. The 2004 Toyota hybrid system is used as a baseline for the comparison. A CR-IM, that produces the same continuous performance as the baseline 50kW IPM motor, has been designed. The cooling system and outer diameter are kept consistent between the competing topologies and hence the stack length is increased for the CR-IM design. The comparative size, weight and parts cost of the designs are presented. The efficiencies and losses of both designs are analysed across the US06, UDDS and HWFET driving cycles and the difference in energy cost over the 120,000 mile vehicle lifetime is calculated. Finally the impact on battery sizing and inverter VA rating is discussed.

The authors would like to thank the International Copper Association for support of this research project.

J. Goss, M. Popescu and D. Staton are with Motor Design Ltd, Ellesemere, UK. (e-mail: info@motor-design.com)

II. 2004 TOYOTA PRIUS ELECTRIC DRIVE SYSTEM

The hybrid system employed in the 2004 Toyota Prius consists of two permanent magnet electrical machines MG1 (Motor/Generator), MG2 and an internal combustion engine (ICE) connected through a planetary gear set. The ICE is a 1.5L 57kW Atkinson cycle petrol engine [1]. The planetary gear set enables the speed of the ICE to be decoupled from the vehicle speed, the purpose of which is to allow the ICE to run at high efficiency operating points and enable charging of the battery pack while the vehicle is stationary [2]. MG1 is a smaller permanent magnet electrical machine that acts mainly as a generator to charge the battery pack through energy taken from the output of the ICE; MG1 also acts as the starter motor for the ICE. MG2 is a larger 50kW IPM motor, the speed of MG2 is directly coupled to the vehicle wheel speed, and the torque provided to the wheels is the sum of the torque from MG2 and the ICE minus the torque taken from the ICE by MG1. MG2 is also used to recover the energy from braking; it is controlled to apply the braking torque up to its maximum torque capability. By controlling MG1 and MG2 the hybrid powertrain acts as an electronically controlled continuously variable transmission. This study evaluates the impact of replacing MG2 with a copper rotor induction motor.

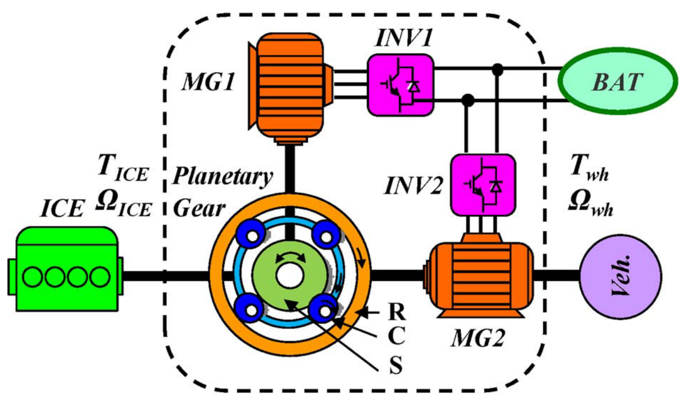

Fig 1- Toyota Prius Hybrid System Diagram [3]

The contribution of MG2 to the output torque is dependent on the vehicle control strategy and the battery management system which utilises information about the battery state of charge (SoC) and the optimal efficiency operating regions of the ICE [4]. For this analysis it is assumed that MG2 supplies 30% of the motoring torque across the driving cycle and recovers any braking torque up-to 250Nm, at which point the frictional brakes supply the rest. However, in reality this power split depends greatly on the mode of operation and can vary from 100% in electric only mode to 0% during low power cruising while the braking torque split is also more complex. Hence the figure we use here is intended to be no more than an aggregate. These simplified assumptions are used to conduct this study.

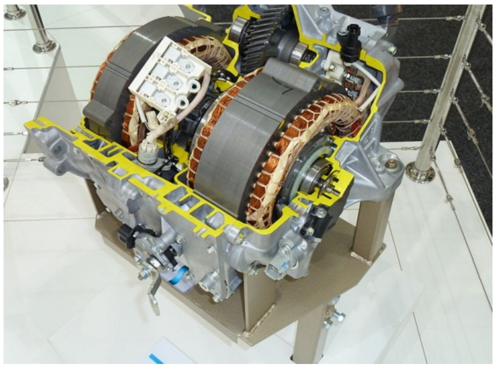

Fig. 2-Toyota Prius Hybrid System [1]

III. COMPARISON OF MACHINE DESIGNS

The baseline design is an 8 pole 48 slot IPM motor with V-magnets and a distributed stator winding. The motor cross-section is shown in fig 3. This design has been electromagnetically and thermally modeled using SPEED [5] and Motor-CAD [6], these models have been calibrated against test results supplied in [1]. Motor-LAB software [7] is used to compute the maximum torque/amp operating point at every driving cycle condition, evaluate the losses over the cycles and generate the efficiency maps.

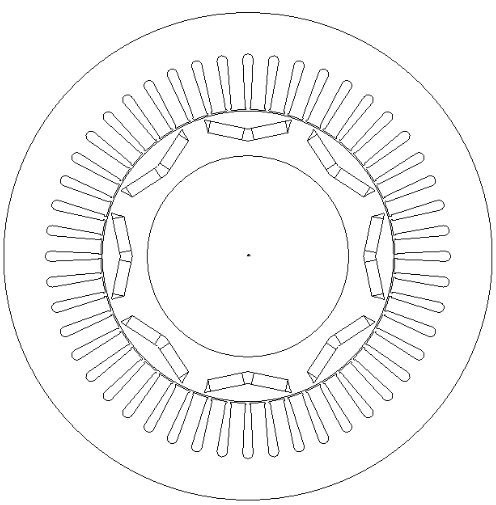

Fig. 3- Baseline IPM Design

The CR-IM has been designed to achieve the same continuous torque and performance envelope as the baseline IPM motor. A 48 slot 62 bar design has been chosen, the cross-section is shown in fig 4. The outer diameter and cooling system has been kept consistent between the two designs, as an induction motor has inherently lower torque density than a permanent magnet motor the CR-IM design requires an increased active length. This gives a larger surface area to extract the loss through the cooling system and also reduces the copper loss improving the efficiency.

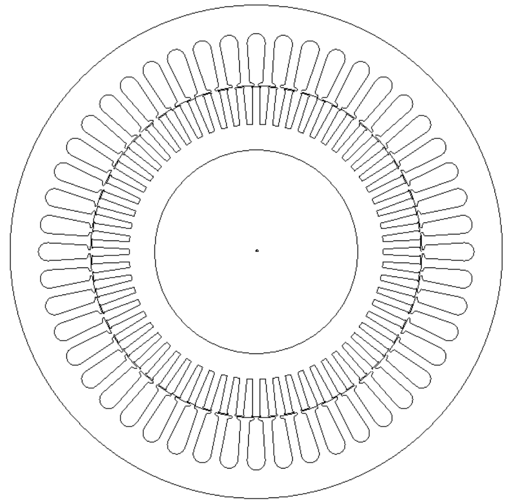

Fig. 4-Alternative CR-IM Design

Using the same modeling tools and assumptions as the experimentally calibrated IPM motor models the stack length of the CR-IM design has been chosen to match the IPM motor steady-state winding temperature at this calibrated operating point. The results are shown in table I; the CR-IM has a 105mm active length compared to 84mm for the baseline IPM motor design.

TABLE I
PERFORMANCE AT CONTINUOUS OPERATING LIMIT

	IPM	*CR-IM*
Stack Length (mm)	84	105
Speed (rpm)	900	900
Torque (Nm)	118	118
Efficiency (%)	92.5	88.2
Total Losses (W)	897	1485
Coolant Temperature	105	105
Maximum Winding Temperature	156	156

Table II shows the breakdown of the materials and costs associated with each design. The active weight of the IPM is 29.7kg while the CR-IM is 41.5kg. The IPM cost has been evaluated using 2011 and 2013 peak NeFeB prices to reflect the market volatility. It can be seen that dependent on the cost of rare-earth magnet material a CR-IM topology reduces the manufacturer material costs by $110-$445 and reduces the consumer purchase price of a vehicle by an estimated $275-$1112.

TABLE II
MATERIAL QUANTITIES AND COSTS

	IPM	*CR-IM*
Copper (kg)	4.5	9.1
Steel (kg)	23.9	24
Permanent Magnet/Rotor Cage (kg)	1.3	8.4
Total (kg)	29.7	41.5
Copper ($)	31.3	63.8
Steel($)	23.9	24.0
Permanent Magnet/Rotor Cage ($)		
2011 NeFeB Price ($400/kg)	536	58.6
2013 NeFeB Price ($150/kg)	201	
Total ($)	256-591	146
Reduction in Consumer Purchase Price with a CR-IM ($)	275-1112	

A motoring efficiency map has been calculated for the IPM motor, fig.5 and the CR-IM fig.6. The peak efficiency is approximately 4% higher in the IPM motor.

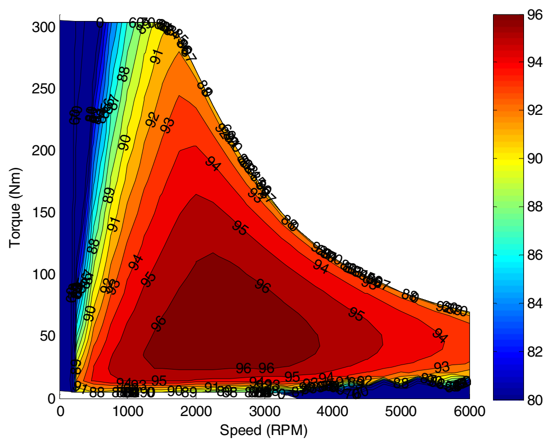

Fig 5- IPM Motoring Efficiency Map

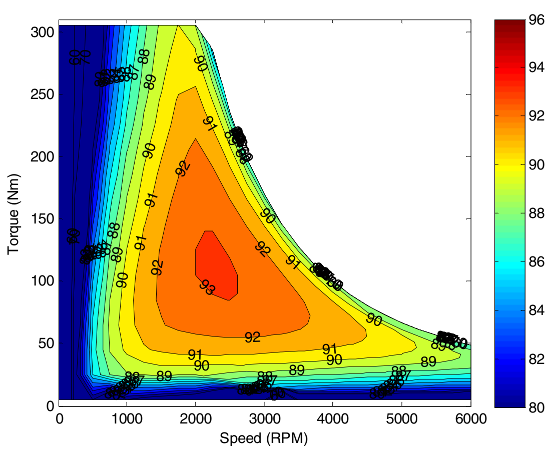

Figure 6- CR-IM Motoring Efficiency Map

IV. DRIVING CYCLES AND VEHICLE MODEL

The driving cycles used in the analysis are the industry standard UDDS- city, HWFET- Highway and US06-Heavy Acceleration cycles, table III. The required operating points are calculated using a simplified steady state vehicle model that takes into account aerodynamic resistance (1), rolling resistance (2) and acceleration (3) assuming a 0% gradient throughout the cycle and no headwind. The motor/generator torque and speed is then calculated using (4) and (5) respectively. The parameters used for the vehicle model are given in table IV.

TABLE III
COMPARISON OF DRIVING CYCLES

	UDDS	*US06*	*HWFET*
Distance (Miles)	7.5	8.01	10.3
Average Speed (mph)	19.6	48.4	48.3

TABLE IV
TOYOTA PRIUS VEHICLE MODEL PARAMETERS

`	*Symbol*	*Value*	*Unit*
Mass	m	1360	kg
Wheel Radius	r_w	0.3	m
Frontal Area	A_f	1.746	m^2
Rolling Resistance Co-efficient	k_R	0.0054	
Drag Co-efficient	C_d	0.26	
Final Drive Ratio	n_d	4.113	
Mass Correction Factor	δ	1.04	

$$F_d = \frac{1}{2}\rho v^2 C_d A_f \tag{1}$$

$$F_r = k_r m g \tag{2}$$

$$F_a = m a \delta \tag{3}$$

$$T_{motor} = \frac{(F_d + F_r + F_a) r_\omega}{n_d} \tag{4}$$

$$\Omega_{motor} = \frac{60 n_d v}{2\pi r_w} \tag{5}$$

Where ρ is the air density, g acceleration due to gravity, v the velocity of the vehicle in m/s, T_{motor} the motor/generator torque in Nm and Ω_{motor} the motor/generator shaft speed in rpm.

Combining the vehicle model and the control strategy described in section II the operating points across the three drive cycles are calculated and shown in figs. 7-9.

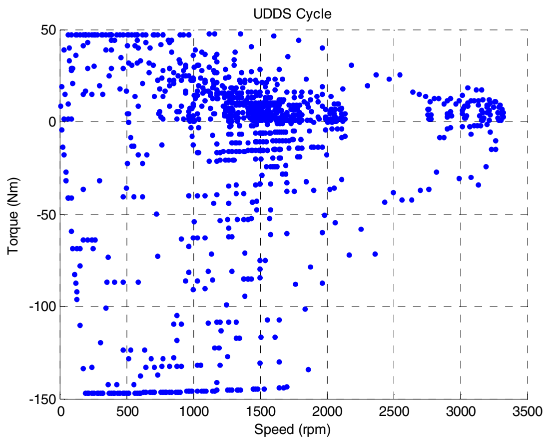

Figure 7- Motoring/Generating Points over the UDDS Cycle

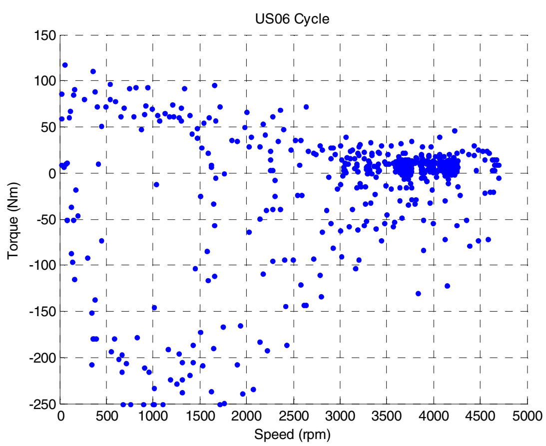

Figure 8-Motoring/Generating Points over the US06 Cycle

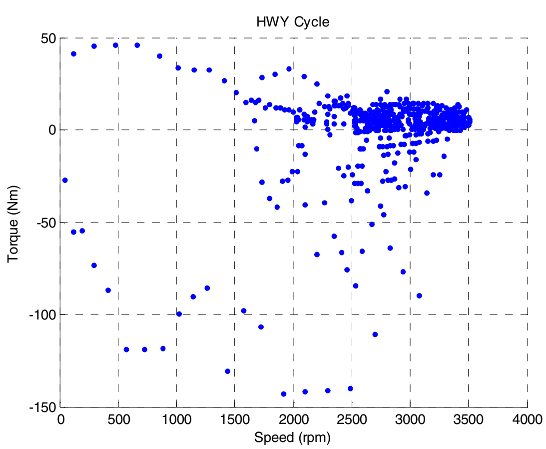

Figure 9- Motoring/Generating Points over the HWFET Cycle

The losses associated with each point for both the IPM and CR-IM designs are then solved and the cumulative energy loss is calculated for each cycle.

V. DRIVE CYCLE ANALYSIS RESULTS

The cumulative loss for the UDDS, US06 and HWFET cycle for the IPM and CR-IM are shown in Figs. 10-12.

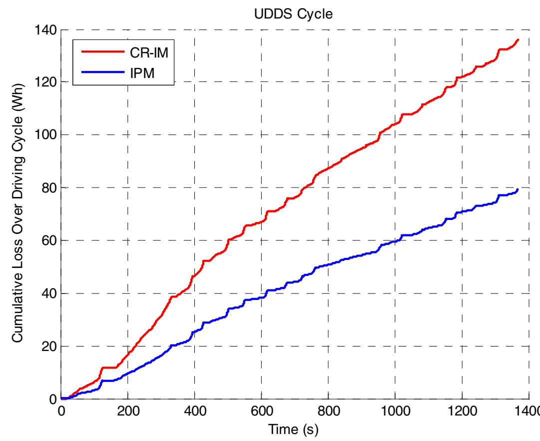

Figure 10-Cumulative Losses over the UDDS Cycle

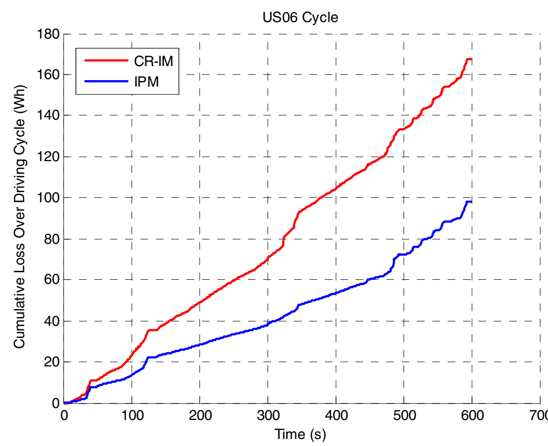

Figure 11-Cumulative Losses over the US06 Cycle

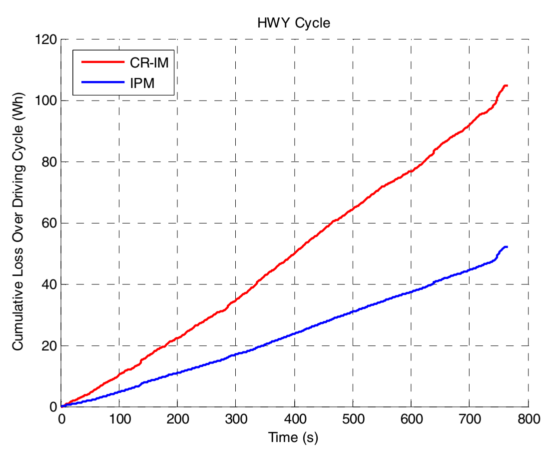

Figure 12-Cumulative Losses over the HWFET Cycle

The CR-IM cumulative losses are larger than the IPM by a factor of 1.6-2 depending on the cycle. The vehicle lifetime is estimated at 120000 miles and the lifetime energy loss for each cycle is shown in table V. The combined average value assumes an equal proportion of each cycle and shows that the

CR-IM uses 895kWh more energy over the vehicle lifetime. Using a typical electricity cost of $0.25/kWh this equates to an extra $224. If this energy is replaced using an ICE as is the case in the baseline system, assuming a petrol price of $1/litre and a 35% ICE efficiency, the CR-IM increases the lifetime fuel cost by $263.

TABLE V
CUMULATIVE LOSSES OVER THE VEHICLE LIFETIME

	IPM	*CR-IM*
UDDS (kWh) over lifetime	1274	2235
US06 (kWh) over lifetime	1430	2514
HWY (kWh) over lifetime	609	1248
Combined Average	1104	1999
Additional Energy Cost from baseline		
@ $0.25/kWh	0	$224
@$0.294/kWh (From ICE)	0	$263

VI. System Impacts

A. Battery Sizing

If a CR-IM is adopted over an IPM topology for a plug-in hybrid or pure electric vehicle the reduced efficiency is likely to result in a reduced range if the battery size remains unchanged. The reason for this is that comparatively more energy will be extracted from the battery to provide the same motor shaft power and less energy will be recovered to the battery during regenerative braking. Therefore to achieve the same specified range with a CR-IM topology in a plug-in hybrid or pure electric vehicle a larger battery capacity will be required.

The battery sizing design decision in a power split hybrid is less obvious however it is likely that reduced motor efficiency will have a similar impact on battery capacity. To make some estimation of the increased battery capacity required with a CR-IM the energy taken and recovered to the battery when 100% of the motoring and braking torque is supplied by the motor/generator during the highway cycle is calculated for each topology. This cycle has been chosen as the low motoring and braking torques can be supplied within the machine envelope without any power assistance from the ICE.

The result of this calculation shows that the IPM topology uses 7% less energy than the CR-IM during braking and recovers 6% more energy than the CR-IM during generating. The total regenerative braking energy over the cycle is 1/5th of the motoring energy. Therefore 9% more energy is required from the battery when a CR-IM is used to achieve the same range. If we assume that 75% of battery energy is used to power the drive train while the other 25% is used on auxiliary systems such as air conditioning, heating and lighting then the battery capacity needs to be increased by approximately 7% to maintain the range when a CR-IM is used in a plug-in or pure battery electric vehicle.

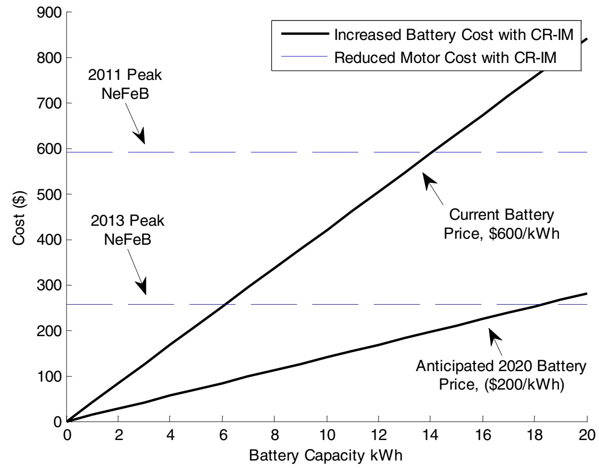

Figure 13-Impact of Battery Capacity on Cost Benefit of CR-IM

Fig.13 shows the increased cost of the battery pack with a CR-IM using a current $600/kWh manufacturer price and an anticipated 2020 price of $200/kWh against the vehicle battery capacity. Also included on the plot is the reduction in motor cost when a CR-IM topology is adopted. Using current prices for NeFeB and the battery pack the CR-IM topology reduces overall system costs when the battery capacity is lower than 6kWh. The battery capacity in the 2004 Toyota Prius hybrid system is 1.2kWh.

B. Inverter VA Rating

Induction motors typically have a reduced power factor and hence higher inverter VA rating than their PM counterparts. Fig.14 shows a motoring power factor map for the CR-IM design and Fig.15 shows a motoring power factor map for the IPM design. At maximum torque and hence current the CR-IM power factor is 0.6 while the PM is 0.7. Therefore the VA rating of the inverter will need to be 10% higher when the CR-IM topology is used.

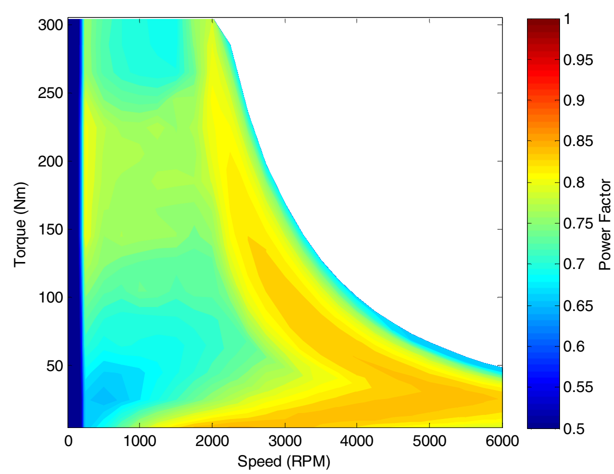

Figure 14-CR-IM Motoring Power Factor Map

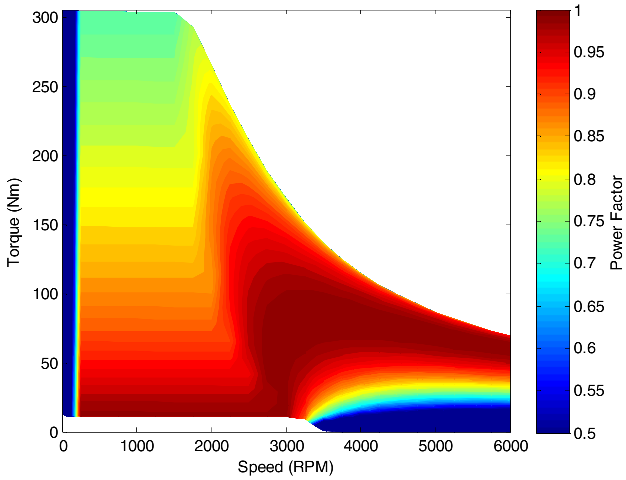

Figure 15-IPM Motoring Power Factor Map

VII. CONCLUSION

For electric and hybrid vehicle traction a copper rotor induction motor offers a low cost alternative to a permanent magnet motor and is immune to the price volatility of rare-earth materials. However their lower efficiency results in a heavier design, slightly higher vehicle running costs, an increased inverter VA requirement and may require an increased battery capacity. Therefore the choice of motor/generator topology requires a careful trade-off between system components. For power split or mild hybrid vehicle applications where battery capacities are low and initial purchase costs are important the CR-IM topology may be advantageous.

REFERENCES

[1] R. H. Staunton, C. W. Ayers, L. D. Marlino, J. N. Chiasson, and T. A. Burress, "Evaluation of 2004 Toyota Prius hybrid electric drive system," U.S. Dept. Energy, Special Rep., May 2006.

[2] C. Mansour and D. Clodic, "Dynamic modeling of the electro-mechanical configuration of the Toyota Hybrid System series/parallel power train," *International Journal of Automotive Technology*, vol. 13, no. 1, pp. 143–166, Oct. 2011.

[3] Y. Cheng, R. Trigui, C. Espanet, A. Bouscayrol, and S. Cui, "Specifications and Design of a PM Electric Variable Transmission for Toyota Prius II," *IEEE Transactions on Vehicular Technology*, vol. 60, no. 9, pp. 4106–4114, Nov. 2011.

[4] E. Vinot, J. Scordia, R. Trigui, B. Jeanneret, and F. Badin, "Model simulation, validation and case study of the 2004 THS of Toyota Prius," *International Journal of Vehicle Systems Modelling and Testing*, vol. 3, no. 3, pp. 139–167, 2009.

[5] T. J. E. Miller, *SPEED's Electric Machines*. 2011.

[6] Motor Design Ltd., "Motor-CAD v7.5 Software." 2012. www.motor-design.com

[7] Motor Design Ltd., "Motor-LAB v1.2 Software." 2013. www.motor-design.com